



# *Cola rostrata* K. Schum. constituents induce cytotoxicity through reactive oxygen species generation and mitochondrial membrane depolarisation

Babatunde E. Ajayi<sup>1,2,3\*</sup> , Bola Oboh<sup>1</sup> , Joseph B. Minari<sup>1</sup> , Darren W. Sexton<sup>4</sup> , Satyajit D. Sarker<sup>3</sup> , Amos A. Fatokun<sup>3\*</sup> 

<sup>1</sup>Department of Cell Biology and Genetics, Faculty of Science, University of Lagos, Akoka, Lagos, Nigeria

<sup>2</sup>Department of Biochemistry, Faculty of Natural and Applied Sciences, Hallmark University, Ijebu-Itele, Ogun State, Nigeria

<sup>3</sup>Centre for Natural Products Discovery (CNPD), School of Pharmacy and Biomolecular Sciences, Faculty of Science, Liverpool John Moores University, L3 3AF Liverpool, UK

<sup>4</sup>School of Pharmacy and Biomolecular Sciences, Faculty of Science, Liverpool John Moores University, L3 3AF Liverpool, UK

**\*Correspondence:** Babatunde E. Ajayi, Department of Cell Biology and Genetics, Faculty of Science, University of Lagos, Akoka, Lagos, Nigeria. [tobitune@yahoo.com](mailto:tobitune@yahoo.com); Amos A. Fatokun, Centre for Natural Products Discovery (CNPD), School of Pharmacy and Biomolecular Sciences, Faculty of Science, Liverpool John Moores University, Liverpool L3 3AF, UK. [A.A.Fatokun@ljmu.ac.uk](mailto:A.A.Fatokun@ljmu.ac.uk)

**Academic Editor:** Katrin Sak, NGO Praeventio, Estonia

**Received:** March 10, 2023 **Accepted:** July 27, 2023 **Published:** December 28, 2023

**Cite this article:** Ajayi BE, Oboh B, Minari JB, Sexton DW, Sarker SD, Fatokun AA. *Cola rostrata* K. Schum. constituents induce cytotoxicity through reactive oxygen species generation and mitochondrial membrane depolarisation. *Explor Target Antitumor Ther.* 2023;4:1328–44. <https://doi.org/10.37349/etat.2023.00200>

## Abstract

**Aim:** While the traditional use of *Cola rostrata* in treating illnesses and diseases has not been reported, the presence of cytotoxic principles has been reported in phylogenetically and biogeographically related species within the *Cola* genus. This study, therefore, evaluated the cytotoxic potential of extracts of the plant, and the associated cellular and molecular mechanisms.

**Methods:** Activity-based fractionation of the extracts was carried out and cytotoxicity was assessed in the human cervical cancer cell line, HeLa, and the transformed human lung cell line, MRC5-SV2, using the 3-(4,5-dimethylthiazol-2-yl)-2,5-diphenyltetrazolium bromide (MTT) assay complemented with brightfield imaging. The 2',7'-dichlorofluorescein diacetate (DCFDA) assay was used to assess induction of cellular reactive oxygen species (ROS), while flow cytometry of 5,5',6,6'-tetrachloro-1,1',3,3'-tetraethylimidacarbocyanine iodide (JC-1)-stained cells assessed the loss of mitochondrial membrane potential ( $\Delta\Psi_M$ ). Gas chromatography-mass spectrometry (GC-MS) analysis was carried out on an active fraction.

**Results:** Extracts of the fruit epicarp and leaf were cytotoxic against the cell lines. Half-maximal inhibitory concentration ( $IC_{50}$ ) values for the 48 h cytotoxicity of the ethanol extract of the epicarp against HeLa and MRC5-SV2 cells were  $48.0 \mu\text{g/mL} \pm 12.1 \mu\text{g/mL}$  and  $40.4 \mu\text{g/mL} \pm 7.2 \mu\text{g/mL}$ , respectively, while fractions from second-level partitioning of the hexane fraction of the leaf extract elicited cytotoxicity with  $IC_{50}$  values ranging from  $12.8 \mu\text{g/mL} \pm 1.0 \mu\text{g/mL}$  to  $39.6 \mu\text{g/mL} \pm 7.2 \mu\text{g/mL}$  in both cell lines, following 48 h treatment. GC-MS revealed the presence of seventeen compounds in a hexane fraction of the leaf extract, including even- and odd-chain fatty acids, the most abundant of which were *n*-hexadecanoic acid, decanoic

© The Author(s) 2023. This is an Open Access article licensed under a Creative Commons Attribution 4.0 International License (<https://creativecommons.org/licenses/by/4.0/>), which permits unrestricted use, sharing, adaptation, distribution and reproduction in any medium or format, for any purpose, even commercially, as long as you give appropriate credit to the original author(s) and the source, provide a link to the Creative Commons license, and indicate if changes were made.



acid 10-(2-hexylcyclopropyl); and octadecanoic acid. The mechanisms of cytotoxicity of most active fractions involved generation of ROS and mitochondrial membrane depolarisation.

**Conclusions:** The findings show that *C. rostrata* is rich in cytotoxic phytochemicals which could be isolated for developing new anti-cancer agents.

## Keywords

*Cola rostrata*, bioassay-guided fractionation, cytotoxicity, reactive oxygen species, mitochondrial membrane potential

## Introduction

Cancer is a disease characterized by uncontrolled proliferation of cells, deranged cellular metabolism, progressive genetic instability, de-differentiation of cells, and metastasis, which, if not detected early enough and appropriately treated, results in death [1, 2]. Currently, cancer is a leading cause of death globally, owing, in part, to its cellular plasticity and increasing chemoresistance to current, clinically used anticancer drugs [3, 4]. The plethora of unwanted side effects of most chemotherapeutic drugs in use today and their declining effectiveness due to resistance mechanisms in cancer cells have made the discovery of more tolerable anticancer drugs, which are less susceptible to chemoresistance, incumbent and urgent. Natural products—in particular, plants—have been viable sources of chemical leads for anticancer drug development [5]. Random selection for screening, chemotaxonomic and pharmacophylogenetic relatedness to known sources of chemical leads, and ethnobotanical usage are some of the reasons why some plants are selected in screening campaigns for chemical leads identification in drug discovery programmes [6–10].

*Cola rostrata* K. Schum. is a tree crop of the Sterculiaceae family that is widely distributed in Gabon, southern Nigeria, and southwestern Cameroon [11–13]. *C. rostrata*, which has two varieties (yellow or white mesocarp) that grow mostly in the wild and sometimes in farms, produces fruits with crunchy, tasty, edible mesocarp [14–16]. The fruit of the yellow variety has a scaly, rough, yellowish, dark-brown epicarp covering usually one or two locules; the plant has 5–7 sub-sessile, broad, acuminate leaflets with a prominent midrib (Figure 1) [17].

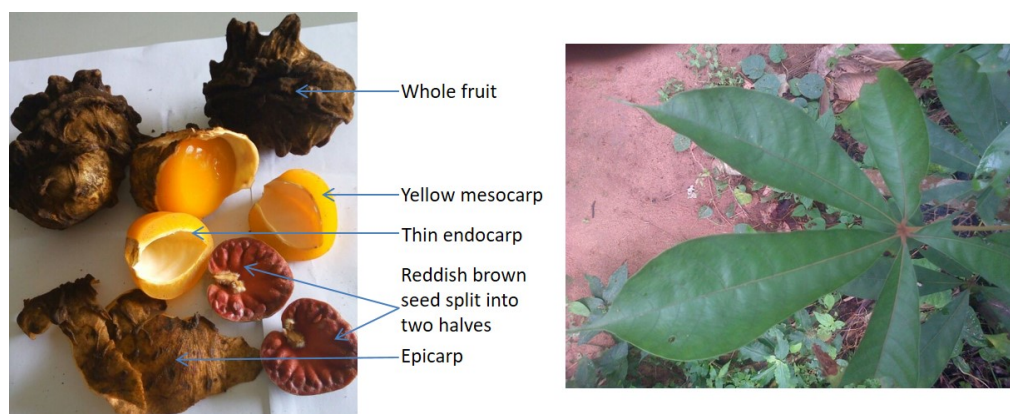


**Figure 1.** The fruits (left image) and leaves (right image) of *C. rostrata*

Traditional use of its close varieties *C. lepidota* and *C. pachycarpa* for the treatment of cancer and pharmacological evidence of the cytotoxicity of their extracts against a panel of cancer cell lines have been reported [18, 19]. While there is limited information on the potential of *C. rostrata* as a source of anticancer compounds, its phylogenetic relatedness to *C. lepidota* and *C. pachycarpa* makes it a good candidate for investigation to ascertain its potential as a source of chemical leads for the development of anticancer drugs. Phytochemical analysis has revealed the presence alkaloids, saponins, terpenoids, flavonoids, phenols, steroids, tannins, cardiac glycosides and anthraquinones in parts of the plant [15, 20]. The fruit epicarp was reported to contain polyphenols, tannins and antimetabolites such as hydrocyanic acid, phytic

acid and oxalic acids; and its extract inhibited the growth of *Escherichia coli*, *Staphylococcus aureus*,  $\beta$ -haemolytic *Streptococcus* and *Klebsiella pneumonia* [21]. A recent paper by the authors reported the presence of drug-like compounds in the fractions of ethanol extract of *C. rostrata* epicarp, which have protein targets that suggest the importance of the epicarp as a potential source of chemical agents for drug development for the treatment of diabetes, pain and inflammatory diseases, and cancer [22].

This study, therefore, examined the cytotoxic potential of ethanol extracts of the fruit epicarp and leaf of *C. rostrata*, using two human cell lines: a cervical cancer cell line, HeLa, and a transformed lung cell line, MRC5-SV2. The extracts were subjected to bioassay-guided fractionation, followed by elucidation of some of the mechanisms of cytotoxic action, and gas chromatography-mass spectrometry (GC-MS) analysis of one of the active fractions.

## Materials and methods

### Plant materials

Plant materials, the fruit and leaf samples, were obtained fresh from the trees at Utu Ikot-Essien, Ikot Ekpene Local Government Area of Akwa-Ibom State, southern Nigeria, between May and August 2018. The samples were authenticated by Professor Abiodun Ayodele of the Department of Botany, University of Ibadan, and the leaf sample specimen was deposited at the University of Ibadan Herbarium, with the voucher number UIH22970.

### Reagents and cell culture materials

Items and their sources included the following: Dulbecco's Modified Eagle Medium (DMEM) (Thermo Fisher Scientific, UK); antibiotic-antimycotic (anti-anti) solution (Thermo Fisher Scientific, UK); foetal bovine serum (FBS; Sigma-Aldrich); L-glutamine (Thermo Fisher Scientific, UK); TrypLE (Thermo Fisher Scientific, UK); 3-(4,5-dimethylthiazol-2-yl)-2,5-diphenyltetrazolium bromide (MTT; Sigma-Aldrich); silica gel—pore size 60 Å 70–230 mesh 63–200 µm (Sigma-Aldrich); silica gel 60H (Merck, Germany); strata C18-E 55 µm, 70 Å 20 g/60 mL (Phenomenex); Dulbecco's phosphate-buffered saline (D-PBS; Thermo Fisher Scientific, UK); 2',7'-dichlorofluorescein diacetate (DCFDA); Reactive Oxygen Species (ROS) Assay Kit (Abcam); JC-1 solid (Sigma-Aldrich); black, microclear 96-well plates (Greiner Bio-One, UK).

### Preparation of extracts

*C. rostrata* leaves and fruit epicarp were air-dried separately under shade at ambient room temperature. The dried materials were cut into small pieces and pulverized with a blender. The leaf and epicarp materials were separately soaked in absolute ethanol for 6 days. The mixtures were vigorously shaken at regular intervals; the extracts were filtered and concentrated. The leaf extract was evaporated to dryness at 45°C, while the epicarp extract was air-dried in a regulated flow cupboard. The samples were labelled 2A and 1A, respectively.

### Cell culture

Immortalised human cervical adenocarcinoma (HeLa) and immortalised, SV40-transformed human lung fibroblast (MRC5-SV2) cells used in the study were originally obtained from the European Collection of Authenticated Cell Cultures (ECACC). The cells were grown as adherent monolayer cultures in T75 flasks or multi-well plates using, as growth medium, DMEM (with phenol red) containing 4.5 g/L glucose, supplemented with 10% FBS, 2 mmol/L L-glutamine, and 1% antibiotic-antimycotic solution was used. The cells were cultured in T75 flasks and incubated in a humidified atmosphere of 37°C and 5% CO<sub>2</sub>; they were prepared and used as described by Omondi et al. [23].

### Treatment of cells with extracts

HeLa and MRC5-SV2 cells were separately prepared at densities  $1 \times 10^5$  cells/mL,  $7.5 \times 10^4$  cells/mL and  $5 \times 10^4$  cells/mL and seeded into 96-well plates (100 µL per well) for 24 h, 48 h and 72 h treatments, respectively. Stock solution (50 mg/mL) of each of the two crude extracts was prepared in dimethyl

sulfoxide (DMSO). The seeded cells were allowed to attach for 24 h and then treated with the extracts, up to 72 h, at final concentrations of 10, 50, 100 and 200 µg/mL, each in triplicate. The final percentage of DMSO (v/v) in the growth medium was less than 0.4%, which was not toxic to the cells. Each treatment was run at least three independent times. Cell morphology changes induced by the treatments were viewed with an Olympus CKX41 microscope fitted with an Olympus DP71 U-TVIX-2 camera and the images were captured with the Olympus cellSens entry 1.16 imaging software.

### Cell viability assay

Cell viability was assessed using the MTT assay as previously reported [23]. To each treatment well in the 96-well plate (clear, flat bottom), 10 µL of a 5 mg/mL MTT solution prepared in phosphate-buffered saline (PBS; pre-warmed to 37°C) was added. The cells were then incubated for 2 h to allow them to convert the MTT into purple-coloured formazan. Afterwards, the liquid content of each well was carefully aspirated to leave only the formazan crystals in the wells. DMSO (100 µL) was added to each of the wells to dissolve the crystals. The plates were shaken on a rotary shaker for approximately 5 min to ensure complete dissolution of the crystals and to achieve a homogeneous solution. Absorbance was then read at 570 nm using the CLARIOstar microplate reader (BMG LABTECH, UK).

### Fractionation of extracts

Extracts 1A and 2A were subjected to solvent partitioning using a separatory funnel. 1A (0.86 g) was partitioned in 60 mL 70% methanol and 40 mL *n*-hexane; the sub-fractions were concentrated under nitrogen using a techne sample concentrator which was regulated to 45°C and air-dried. The polar sub-fraction was labelled 1AM, while the non-polar sub-fraction was labelled 1AFK. 2A (8.74 g) was partitioned in two batches between 70% methanol and *n*-hexane; each batch had a total volume of 300 mL in a ratio 2:1 (70% methanol:*n*-hexane). The polar sub-fraction was concentrated under nitrogen, air-dried and labelled 2AFM. The non-polar sub-fraction had a component which partitioned with it but remained undissolved; the sub-fraction was filtered and the filtrate was concentrated, air-dried and labelled 2AFH. The undissolved fraction was found to be soluble in ethyl acetate, and the sub-fraction obtained therefrom was filtered, air-dried and labelled 2AFU.

Based on the cytotoxicity assays, 2AFH (1.5 g) was separated using vacuum liquid chromatography (VLC) and eluted with a mobile phase composed of varying proportions of *n*-hexane and ethyl acetate: 100% *n*-hexane, 95:5, 90:10, 75:25, 60:40, 50:50, 40:60, 20:80 and 100% ethyl acetate; the fraction left in the column was eluted with 100% methanol. The 100% *n*-hexane and 5% ethyl acetate in *n*-hexane did not elute any significant amount of the extract, and the remaining sub-fractions were labelled 2AFH10, 2AFH25, 2AFH40, 2AFH50, 2AFH60, 2AFH80, 2AFH100 and 2AFH100MeOH, respectively. 2AFH40 was further separated using column chromatography and eluted with a mobile phase comprising various ratios of *n*-hexane and ethyl acetate from 100% *n*-hexane to 100% ethyl acetate. The fractionation schemes for crude extracts 1A and 2A are shown in [Figure 2](#).

### DCFDA cellular ROS assay

To determine aspects of the mechanisms of cytotoxicity of the extract fractions, potential generation of intracellular ROS was assessed using the DCFDA Cellular ROS Detection Assay Kit (Abcam, catalogue number ab113851) according to the manufacturer's protocol and as previously described [23]. Each extract fraction was dissolved in DMSO and tested on HeLa cells cultured 24 h previously at a density of  $2.5 \times 10^5$  cells/mL (100 µL/well in a black, microclear 96-well plate). The final concentrations of each extract fraction tested were 10, 50, 100 and 200 µg/mL (prepared in growth medium without phenol red). The concentrations of the positive control [tert-butyl hydroperoxide (TBHP)] were 100 µmol/L and 200 µmol/L. Fluorescence at 483-14 nm/530-30 nm was recorded from 3 h up to 24 h post-treatment, using the CLARIOstar microplate reader (BMG LABTECH, UK). Background fluorescence was subtracted from each value before fold increase in fluorescence intensity relative to the negative control was determined. The assay was conducted three independent times.

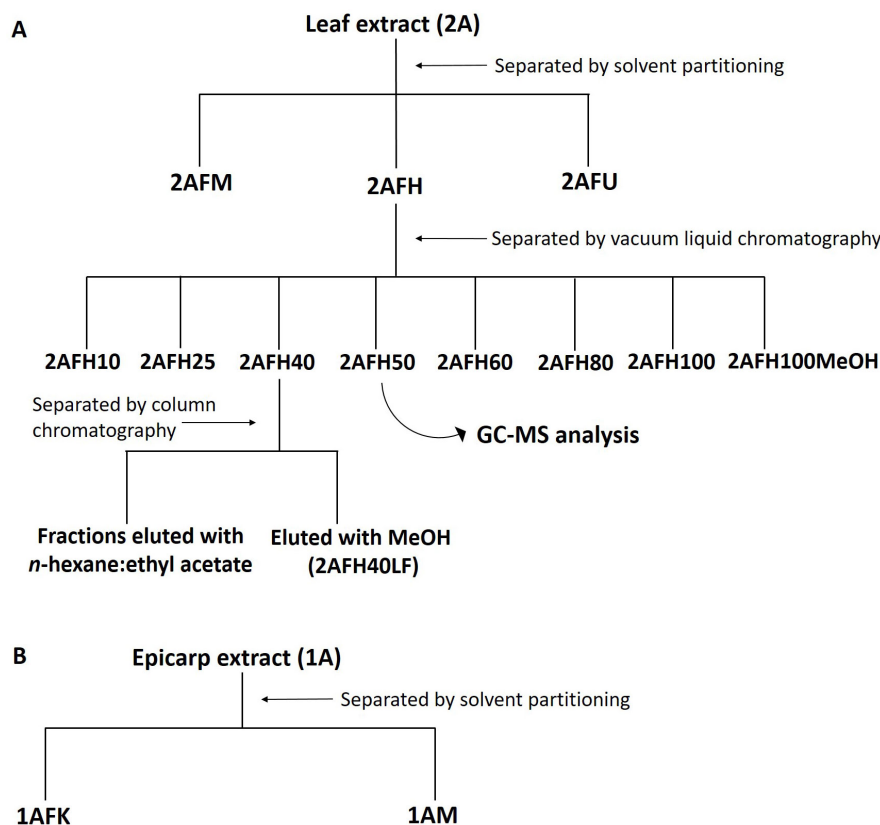


**Figure 2.** Fractionation scheme for ethanol extracts of *C. rostrata* leaf and fruit epicarp. (A) The leaf extract, 2A, had fractions separated by solvent partitioning and chromatographic methods; (B) the epicarp extract, 1A, was separated by solvent partitioning into polar and non-polar fractions

### Mitochondrial membrane depolarization assay (JC-1 staining)

MRC5-SV2 cells were seeded into a 24-well Falcon plate at a density of  $1 \times 10^5$  cells/mL and a volume of 300  $\mu$ L/well. The cells were allowed to attach for 24 h and then examined under the microscope to confirm their attachment and healthy, uncontaminated growth. 2-fold (2 $\times$ ) solutions of 10, 50, 100 and 200  $\mu$ g/mL of 1AFK, 1AM, 2AFH25 and 2AFH50 were prepared from their stock solutions (50 mg/mL in DMSO) using pre-warmed growth medium. From each well, 150  $\mu$ L of growth medium was removed and 150  $\mu$ L of each 2 $\times$  concentration of each extract fraction was added. Fresh growth medium (150  $\mu$ L) was added to two wells which served as the growth medium control wells, and 150  $\mu$ L of growth medium containing DMSO in the same percentage of DMSO (v/v) as it was in the highest test concentration (200  $\mu$ g/mL) was added to two wells which served as the DMSO control wells. The cells were incubated at 37°C for 3 h.

A 1:200 dilution of a 4 mmol/L stock 5,5',6,6'-tetrachloro-1,1',3,3'-tetraethyl-imidacarbocyanine iodide (JC-1) solution in DMSO was prepared in pre-warmed growth medium. Working JC-1 solution (30  $\mu$ L) was added to each well (final concentration 2  $\mu$ mol/L) and the cells were incubated for 1 h at 37°C. The medium in each well (corresponding to a concentration of each test fraction) was aspirated into a labelled Eppendorf tube to collect all suspended cells. PBS (200  $\mu$ L) was used to rinse each well to remove residual growth medium. The PBS was then carefully aspirated, 100  $\mu$ L of TrypLE was added to detach the adherent cells, and the cells were incubated at 37°C for 5 min for complete detachment. Fresh growth medium (100  $\mu$ L) was added to each well to stop the trypsin action; the content of each well was collected into the corresponding Eppendorf tube already containing the suspended cells, and the content was mixed. Fluorescence was determined using a BD Accuri C6 flow cytometer. Morphologically viable and dying cells were gated based on forward and side scatter parameters and to the exclusion of debris. Gated cells were then analysed for monomeric JC-1 green fluorescence (FL1:  $\lambda_{ex}$  488 nm;  $\lambda_{em}$  533/30 nm) and polymeric yellow/orange fluorescence (FL2:  $\lambda_{ex}$  488 nm;  $\lambda_{em}$  585/25 nm). Compensation for FL1 spillover into FL2 was performed and set at 10.54% and a total of 5,000 cell events were collected for each sample. Data was analysed using the instrument's C6 Analysis software.

## GC-MS analysis of active fraction

Fraction 2AFH50 was analyzed on Gas Chromatography (Agilent Technologies, 7890, USA) apparatus coupled with a Mass Spectrometer (Agilent Technologies, 5975, USA). The column (Agilent Technologies, HP5MS) had a length of 30 cm, internal diameter of 0.320 mm and thickness of 0.25  $\mu\text{m}$ . The initial oven temperature was set to 80°C for 2 min, increased at a rate of 12°C per min to 240°C and then held for 6 min. The volume injected was 1  $\mu\text{L}$  and the mode of analysis was splitless. The interface temperature between the Gas Chromatography apparatus and the mass spectrometer was 250°C. The total run time was 22 min and scans ranged from 50 m/z to 500 m/z, and a search of the National Institute of Standards and Technology (NIST) 14 library was used to identify the compounds represented by the peaks.

## Data presentation and statistical analysis

Experiments were conducted at least three independent times, with each treatment for each run assessed at least in duplicate. Except otherwise stated, each experimental value is presented as mean  $\pm$  standard error of the mean (SEM). One-way analysis of variance (ANOVA) followed by post-hoc test (Tukey test) for multiple comparisons was used to determine statistical significance of differences between means, using the GraphPad Prism software (Version 8.0.1; GraphPad Software Incorporated, CA, USA). A  $P$ -value  $< 0.05$  was considered statistically significant.  $\text{IC}_{50}$  value was determined using GraphPad Prism by fitting the data to the non-linear regression "log [inhibitor] versus normalized response".

## Results

### Cytotoxicity of crude extracts

As shown in Figure 3 that depicts the effects of the epicarp extract 1A and Figure 4 that lists the  $\text{IC}_{50}$  values of 1A and the leaf extract 2A, both 1A and 2A were cytotoxic against HeLa and MRC5-SV2 cells when tested within the concentration range 10–200  $\mu\text{g}/\text{mL}$  for up to 72 h. However, the effects were not exposure time-dependent, as most values at 72 h were not significantly different to values at 48 h (Figures 3 and 4). The cytotoxic effect of 1A against both cell lines was significant from 10  $\mu\text{g}/\text{mL}$  and concentration-dependent across 10  $\mu\text{g}/\text{mL}$  and 50  $\mu\text{g}/\text{mL}$  but then peaked at 50  $\mu\text{g}/\text{mL}$  for the HeLa cells (Figure 3A), while generally further decreases in viability beyond that elicited by 50  $\mu\text{g}/\text{mL}$  were modest (48 h) or insignificant (72 h) in the MRC5-SV2 cells (Figure 3B). Over both time points (48 h, 72 h) and against the two cell lines, 1A was approximately three to four times more potently cytotoxic than 2A (Figure 4). There was evidence that morphological damage accompanied the cytotoxicity induced by the extracts, as their higher concentrations caused loss of confluency and shrinkage of most of the remaining cells.

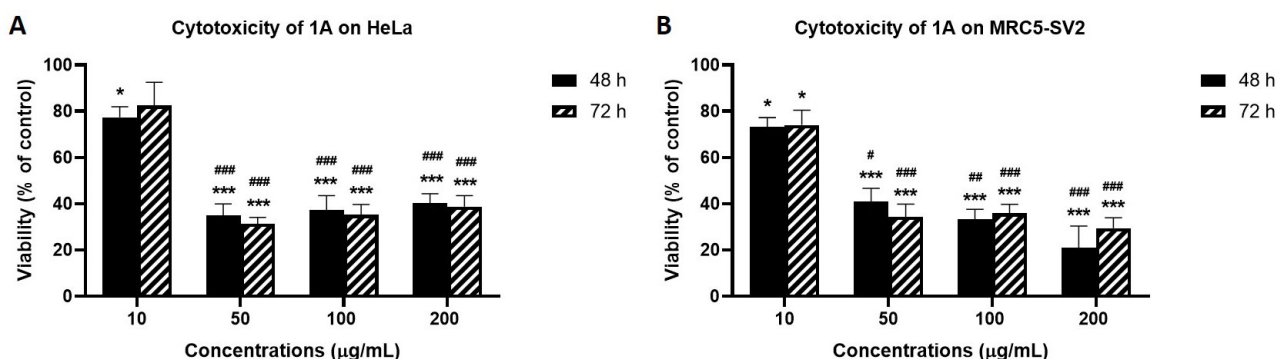


**Figure 3.** Effects of 48 h and 72 h treatments with extract 1A on the viability of (A) HeLa cells, and (B) MRC5-SV2 cells. \*  $P < 0.05$  and \*\*\*  $P < 0.001$  represent significant differences in cell viability between 1A treatment and negative control, while #  $P < 0.05$ , ##  $P < 0.01$  and ###  $P < 0.001$  represent significant differences in cytotoxicity between the indicated concentration and 10  $\mu\text{g}/\text{mL}$  treatment. The experiment was run three independent times ( $n = 3$ )

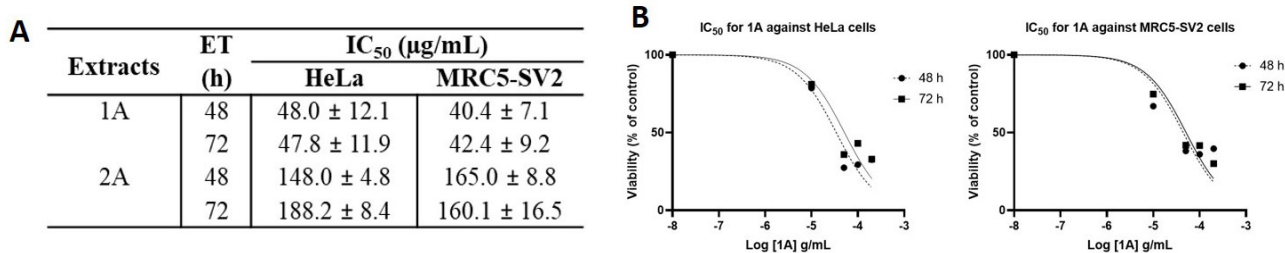


**Figure 4.** Cytotoxic effects of 1A and 2A on HeLa and MRC5-SV2 cells. (A) IC<sub>50</sub> values for the cytotoxicity of 1A and 2A against HeLa and MRC5-SV2 cells; (B) representative concentration-response curves for the cytotoxicity of 1A against HeLa and MRC5-SV2 cells at 48 h and 72 h of treatment. ET: exposure time in hours

### Cytotoxicity of fractions

Solvent partitioning of 2A yielded three fractions: 2AFH, 2AFM and 2AFU; 2AFH and 2AFU each showed significant activity at most of the four concentrations tested, while 2AFM only showed significant cytotoxic ( $P < 0.001$ ) activity at 200 μg/mL against HeLa and MRC5-SV2 cells at 48 h and 72 h time points (Table 1). 2AFH and 2AFU showed concentration-dependent cytotoxicity against both cell lines in all the concentrations tested at 48 h, with significant difference ( $P < 0.001$ ) between the viabilities of the treated wells and those of the negative control wells (Table 1). At the lowest concentration tested (10 μg/mL), surprisingly the 72 h treatment of both cell lines with 2AFH and 2AFU, as opposed to the 48 h treatment, did not reduce the viability of the cells in most cases. The IC<sub>50</sub> values for the cytotoxicities of the three fractions are also shown in Table 1. The effects of 2AFH and 2AFU were generally not time-dependent against both cell lines. In contrast, 2AFM was more cytotoxic against the HeLa cell line in the longer (72 h) time point.

**Table 1.** Cytotoxicity of 2A fractions: 2AFH, 2AFM and 2AFU against HeLa and MRC5-SV2 cells

2A Fractions	Cell line	ET (h)	Cell viability (negative control normalised to 100%)				IC <sub>50</sub> (μg/mL)
			10 μg/mL	50 μg/mL	100 μg/mL	200 μg/mL	
2AFH	HeLa	48	72.3 ± 2.5***	48.7 ± 3.0***	39.0 ± 4.9***	32.7 ± 4.7***	59.4 ± 11.1
		72	104.6 ± 3.3	59.6 ± 2.8***	40.3 ± 3.6***	31.2 ± 1.2***	84.0 ± 6.1
	MRC5-SV2	48	80.4 ± 5.1*	55.3 ± 4.3***	42.1 ± 3.6***	33.3 ± 4.0***	63.2 ± 12.4
		72	104.3 ± 3.9	49.4 ± 6.6***	30.3 ± 5.3***	21.5 ± 3.5***	60.4 ± 11.8
2AFM	HeLa	48	120.6 ± 4.3	120.8 ± 6.8	109.0 ± 2.4	48.2 ± 7.5***	> 700
		72	106.7 ± 5.8	111.4 ± 2.0	78.9 ± 6.5	27.5 ± 3.0***	235.0 ± 17.8
	MRC5-SV2	48	105.0 ± 3.5	115.4 ± 3.7	98.9 ± 5.4	46.6 ± 11.8***	> 500
		72	136.3 ± 15.2	112.8 ± 1.1	100.5 ± 4.2	63.0 ± 3.1***	> 600
2AFU	HeLa	48	74.8 ± 2.0***	60.9 ± 2.7***	50.1 ± 4.1***	41.3 ± 4.3***	99.0 ± 14.2
		72	79.6 ± 4.6**	63.0 ± 3.4***	49.5 ± 3.3***	30.2 ± 3.0***	87.0 ± 10.7
	MRC5-SV2	48	74.3 ± 3.1***	62.1 ± 2.7***	54.5 ± 1.9***	43.8 ± 0.9***	109.0 ± 12.2
		72	106.9 ± 4.4	76.7 ± 1.7*	56.5 ± 4.1***	38.5 ± 4.6***	146.0 ± 17.5

\*  $P < 0.05$ , \*\*  $P < 0.01$ , and \*\*\*  $P < 0.001$  indicate a significant difference between the cell viability of treated cells and the cell viability of untreated cells of the negative control wells. ET: exposure time in hours

Solvent partitioning of 1A gave two fractions: 1AFK (non-polar) and 1AM (polar). 1AFK showed greater cytotoxicity than 1AM on both cell lines, especially at 48 h (Figure 5A and B for HeLa). The photomicrographs (Figure 5C and D) show a reduction in HeLa cell number when the negative control cells (Figure 5C) are compared with the 1AFK (200 μg/mL)-treated cells (Figure 5D), as well as morphological changes to the cells following 24 h treatment with 1AFK. At higher concentrations of 1AFK, dying cells had morphological features consistent with apoptosis, including shrinkage (Figure 5D, see white arrows). 1AFK elicited concentration-dependent and time-dependent cytotoxicity against both cell lines. 1AM showed significant cytotoxicity ( $P < 0.001$ ) against HeLa cells from the 50 μg/mL treatment up to the 200 μg/mL treatment for both 24 h and 48 h. The cytotoxicity of 1AM was, however, generally not significantly

concentration-dependent or time-dependent against HeLa cells (Figure 5B); and it was not concentration-dependent against MRC5-SV2 cells after 48 h (figures not shown). The  $IC_{50}$  values for the cytotoxicity of 1AFK against HeLa and MRC5-SV2 cells are  $122.0 \mu\text{g/mL} \pm 12.0 \mu\text{g/mL}$  and  $132.0 \mu\text{g/mL} \pm 24.4 \mu\text{g/mL}$ , respectively, for the 24 h treatments; and  $81.0 \mu\text{g/mL} \pm 12.7 \mu\text{g/mL}$  and  $52.2 \mu\text{g/mL} \pm 3.5 \mu\text{g/mL}$ , respectively, for the 48 h treatments. For 1AM, the  $IC_{50}$  values for its cytotoxicity are  $134.0 \mu\text{g/mL} \pm 26.4 \mu\text{g/mL}$  and  $114.0 \mu\text{g/mL} \pm 12.7 \mu\text{g/mL}$  for 24 h and 48 h treatments of HeLa cells, respectively; and  $80.1 \mu\text{g/mL} \pm 4.3 \mu\text{g/mL}$  for 48 h treatment of MRC5-SV2 cells.

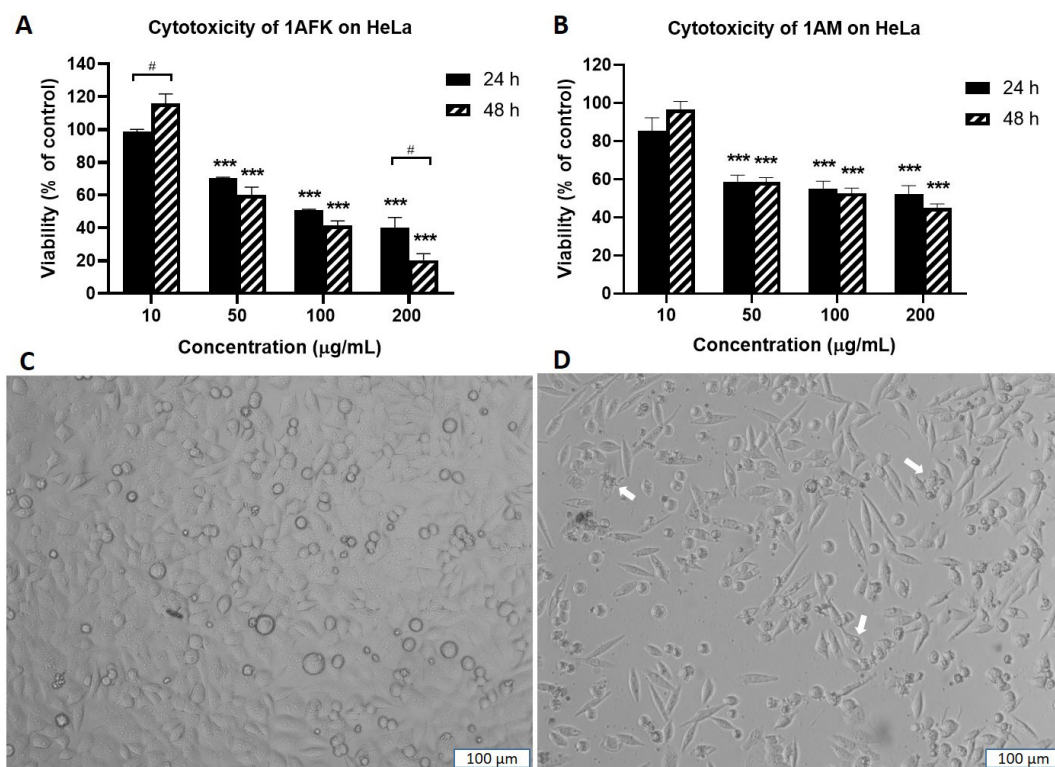


**Figure 5.** Cytotoxicity of fractions 1AFK and 1AM against HeLa cells after 24 h and 48 h treatments. Viability of cells in untreated wells (negative control) was taken as 100%. (A) HeLa cells treated with 1AFK; (B) HeLa cells treated with 1AM; (C) photomicrograph of negative control HeLa cells after 24 h treatment; (D) photomicrograph of HeLa cells treated with 200  $\mu\text{g/mL}$  of 1AFK for 24 h, showing reduced cell number. White arrows point to dying cells with morphological features consistent with apoptosis. \*\*\*  $P < 0.001$  represents a significant difference in cell viability between negative control cells and cells treated with fraction; #  $P < 0.05$  represents a significant difference between 24 h cytotoxicity and 48 h cytotoxicity of the same concentration. Magnification:  $\times 100$ , scale bar: 100  $\mu\text{m}$

### Cytotoxicity of 2AFH fractions

VLC fractionation of 2AFH yielded eight fractions (see Figure 2) with varying levels of cytotoxicity. The yellowish fraction, 2AFH10, was not tested because it was only sparingly soluble in DMSO. 2AFH25 and 2AFH40 were moderately soluble in DMSO when prepared as 50 mg/mL stock solutions, while the remaining fractions were fully soluble. The concentration-dependent (and, in some cases, time-dependent) cytotoxic effects of 2AFH25, 2AFH40 and 2AFH50 are shown in Figure 6 and the  $IC_{50}$  values for the seven fractions (apart from the insoluble 2AFH10) are shown in Table 2. 2AFH60 was nearly equipotent against both cell lines, with 24 h cytotoxicity  $IC_{50}$  values of  $24.6 \mu\text{g/mL} \pm 2.1 \mu\text{g/mL}$  and  $26.4 \mu\text{g/mL} \pm 4.7 \mu\text{g/mL}$ , for HeLa and MRC5-SV2 cells, respectively. 2AFH80 and 2AFH100 significantly reduced the viability of MRC5-SV2 cells, with  $IC_{50}$  values of  $16.4 \mu\text{g/mL} \pm 0.6 \mu\text{g/mL}$  and  $30.9 \mu\text{g/mL} \pm 3.6 \mu\text{g/mL}$ , respectively, after 48 h treatment. 2AFH-derived fractions were generally more toxic than the parent extract. Among the fractions, there was a gradual reduction in cytotoxicity as polarity increased (Table 2). It should be noted that the mass of 2AFH50 obtained was relatively small compared to that of 2AFH40, and 2AFH50 was, therefore, not considered suitable for further fractionation.



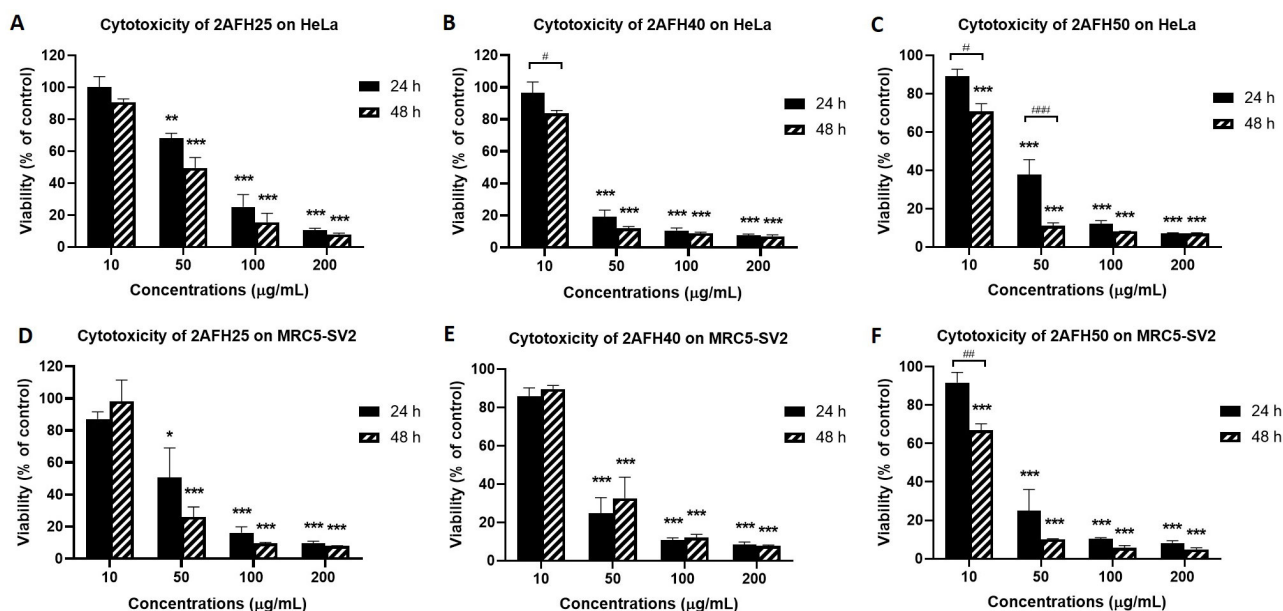


**Figure 6.** Cytotoxicity of some 2AFH fractions against HeLa and MRC5-SV2 cells after 24 h and 48 h treatments. (A, D) Cytotoxicity of 2AFH25 against HeLa and MRC5-SV2 cells; (B, E) cytotoxicity of 2AFH40 against HeLa and MRC5-SV2 cells; (C, F) cytotoxicity of 2AFH50 against HeLa and MRC5-SV2 cells. \*  $P < 0.05$ , \*\*  $P < 0.01$  and \*\*\*  $P < 0.001$  represent a significant difference in cell viability between treatment with fraction and treatment with negative control; #  $P < 0.05$ , ##  $P < 0.01$  and ###  $P < 0.001$  represent a significant difference between 24 h cytotoxicity and 48 h cytotoxicity of the same concentration of the fraction

**Table 2.** IC<sub>50</sub> values for the cytotoxic effects of 2AFH fractions on HeLa and MRC5-SV2 cells following 24 h and 48 h treatments ( $n = 3$ )

2AFH fractions	HeLa (IC <sub>50</sub> , µg/mL)		MRC5-SV2 (IC <sub>50</sub> , µg/mL)	
	24 h	48 h	24 h	48 h
2AFH25	60.9 ± 7.7	39.6 ± 7.2	41.8 ± 12.0	27.9 ± 4.3
2AFH40	25.5 ± 3.4	18.9 ± 0.4	24.6 ± 2.8	26.7 ± 4.7
2AFH50	31.3 ± 4.4	14.9 ± 0.8	26.4 ± 4.5	12.8 ± 1.0
2AFH60	24.6 ± 2.1	18.5 <sup>a</sup>	26.4 ± 4.7	15.9 ± 0.9
2AFH80	24.3 <sup>a</sup>	27.0 ± 6.9 <sup>b</sup>	22.6 ± 3.1 <sup>b</sup>	16.4 ± 0.6
2AFH100	83.2 ± 3.6	35.4 ± 1.2	47.5 ± 1.5	30.9 ± 3.6
2AFH100MeOH	ND	104.0 ± 15.2	ND	80.4 ± 11.2

ND: not determined. <sup>a</sup> value is for  $n = 1$ , and <sup>b</sup> value is for  $n = 2$

### Effects on intracellular levels of ROS

ROS generation in HeLa cells due to exposure to different concentrations of 1AFK, 1AM, 2AFU, 2AFH25, 2AFH50 and 2AFH100MeOH was determined in a bid to identify potential mechanisms of action of the secondary metabolites in the extract fractions that might underlie their cytotoxicity and induction of cell death. TBHP, as positive control, induced concentration-dependent increases in ROS levels at 3, 6, 15 and 24 h exposure time points, peaking at 3 h time point, where at 100 µmol/L and 200 µmol/L it induced 5-fold and 9-fold increases, respectively (Figure 7A). 1AFK induced ROS in a concentration-dependent manner at each of the four time points examined, with 200 µg/mL at 3 h producing nearly a 12-fold increase (Figure 7B).

1AM induced apparently concentration-dependent but largely insignificant ROS production, which at the highest concentration (200 µg/mL) was approximately 2-fold increase for the 3 h time point, an effect that progressively dissipated over the 24 h time period (Figure 7C). The intracellular ROS-generating activity of 2AFU, as depicted in Figure 7D, was not concentration-dependent; at its peak ROS production time point (3 h), the 50 µg/mL, 100 µg/mL and 200 µg/mL treatments each produced an average of about 1.7-fold increase in ROS levels, which progressively reduced to near negative control levels within 15 h following treatment.

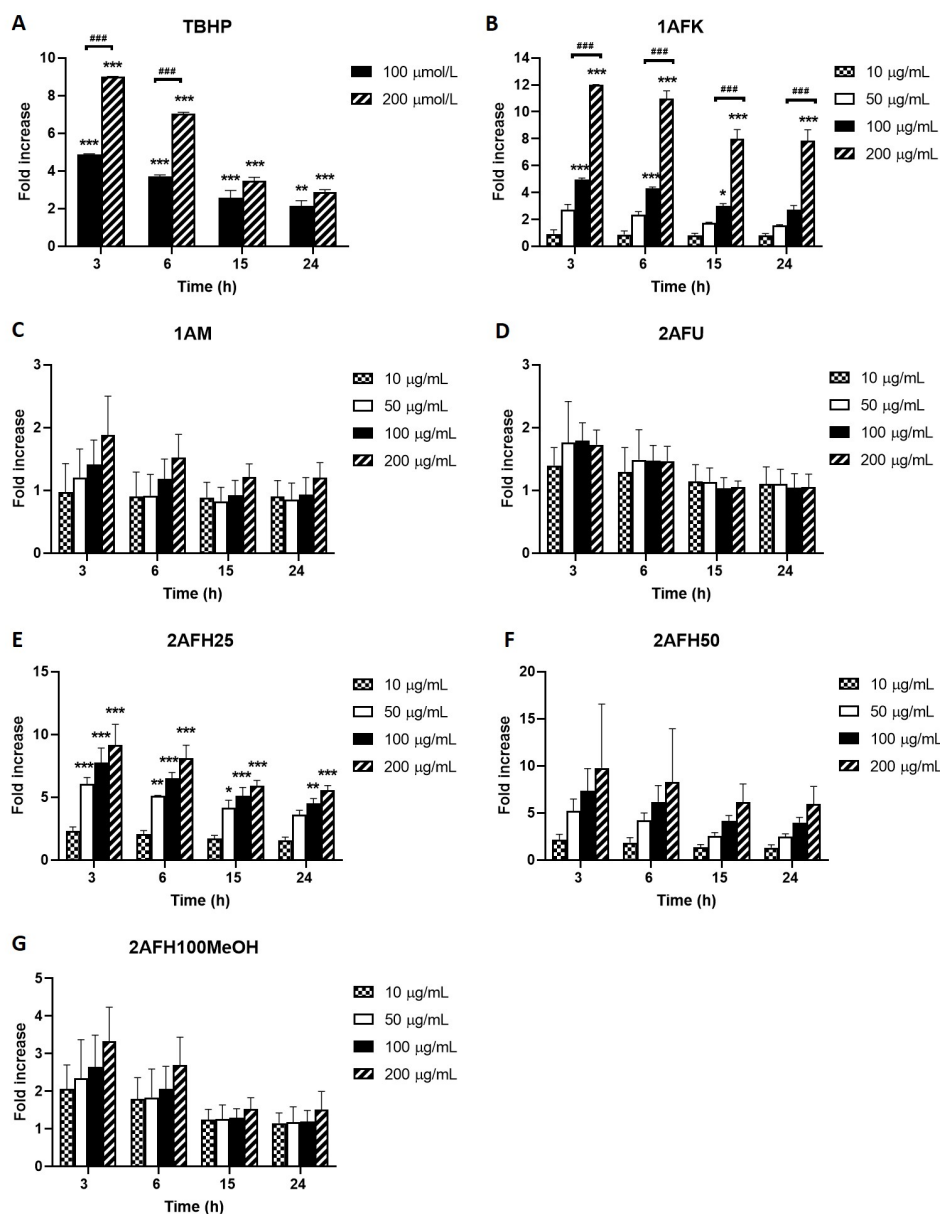


**Figure 7.** Intracellular ROS generation by extract fractions in HeLa cells over a 24 h period (expressed as fold increases compared to the negative control). (A) TBHP (positive control); (B) 1AFK; (C) 1AM; (D) 2AFU; (E) 2AFH25; (F) 2AFH50; (G) 2AFH100MeOH. \*  $P < 0.05$ , \*\*  $P < 0.01$  and \*\*\*  $P < 0.001$  represent a significant difference in intracellular ROS generation between treatment and negative control; ###  $P < 0.001$  represents a significant difference in ROS generation between indicated concentrations of the same extract fraction at the same time point. Each experiment was run three independent times ( $n = 3$ )

2AFH25 and 2AFH50 each induced a concentration-dependent generation of cellular ROS that peaked within 3 h of exposure to them (Figure 7E and F). At the lowest concentration, 10 µg/mL, 2AFH25 and 2AFH50 each produced about a 2-fold increase in ROS levels within 3 h, and at the highest concentration, 200 µg/mL, 2AFH25 produced a 9-fold increase, while 2AFH50 produced a 9.7-fold increase (there was wide variability for 2AFH50 effect). At 24 h, the ROS levels maintained by 2AFH25 and 2AFH50 were about 5.5-folds and 6.4-folds, respectively. 2AFH100MeOH induced concentration-dependent increases in cellular ROS at the 3 h and 6 h time points, beyond which the levels were not different to those of negative control cells (Figure 7G).

### Effects on mitochondrial membrane integrity

HeLa cells were treated with five extract fractions: 1AFK, 1AM, 2AFH25, 2AFH50 and 2AFH40LF at final concentrations of 10, 50, 100 and 200 µg/mL over a 4 h period. 2AFH40LF, the major fraction derived from 2AFH40, was introduced here and in subsequent mechanistic assays in order to compare or contrast the effect of such a downstream fraction with those of the first- and second-level fractions (the  $IC_{50}$  for the

cytotoxicity of 2AFH40LF against HeLa cells after 24 h was  $55.1 \mu\text{g}/\text{mL} \pm 2.7 \mu\text{g}/\text{mL}$ ). The fluorescence of JC-1, a cationic dye which diffuses easily across mitochondrial membrane and accumulates in the negatively charged mitochondrial matrix, was used as a readout for the mitochondrial membrane potential ( $\Delta\Psi_M$ ), which is an index of mitochondrial membrane integrity (mitochondrial health). JC-1 molecules reversibly form aggregates (polymers) in the mitochondria of healthy cells and predominance of the monomers in the mitochondria is indicative of impaired mitochondrial function and initiation of the apoptotic cell death process. The ratio of the count of JC-1 polymers (aggregates) that give high yellow/orange fluorescence and detect healthy cells, to the count of JC-1 monomers that give higher green fluorescence and detect apoptotic cells, was evaluated as a surrogate for  $\Delta\Psi_M$ .

The distribution and count of cells stained with JC-1 which appeared as monomers and polymers for each treatment are displayed in Figure 8. Firstly, Figure 8A shows all sample events in a negative control and the gating, based on forward and side scatter, to eliminate debris and select morphologically viable and apoptotic “cells” for assessment of JC-1 fluorescence. P1, as shown in Figure 8B, represents JC-1-labelled viable cells which have both high green and yellow/orange fluorescence. The population of cells outside of P1 represents cells with depolarized mitochondria and, thus, little polymeric JC-1 (yellow/orange fluorescence). The density plots for 10  $\mu\text{g}/\text{mL}$  and 200  $\mu\text{g}/\text{mL}$  concentrations of the five extract fractions are shown in Figure 8C–L, with 2AFH25, 2AFH40LF and 2AFH50 showing similar patterns of concentration-dependent change, though with different proportions of cells gated in P1. Several plots also depict two populations of depolarized cells with differing levels of green fluorescence, indicative of disrupted JC-1 dye loading into cells and mitochondria. The proportion of cells in P1 area for each of the extract fractions shows a concentration-dependent reduction in population (Figure 9). Based on the proportion of HeLa cells in P1, extract fractions 1AM, 2AFH40LF and 2AFH50 appear to be more efficient at disrupting mitochondrial function even at a concentration as low as 10  $\mu\text{g}/\text{mL}$  within 4 h of treatment.

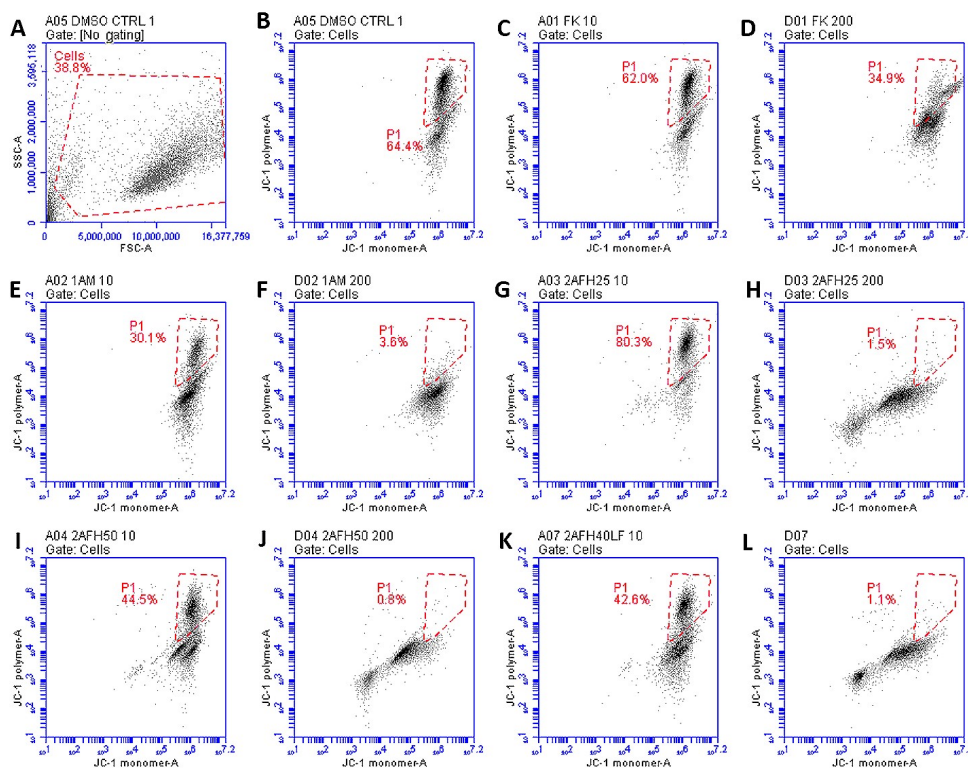


**Figure 8.** Representative density plots of JC-1 staining of HeLa cells following treatment with extract fractions 1AFK (indicated as “FK”), 1AM, 2AFH25, 2AFH40LF and 2AFH50 at 10  $\mu\text{g}/\text{mL}$  and 200  $\mu\text{g}/\text{mL}$  (numerals after each extract designation indicate concentrations in  $\mu\text{g}/\text{mL}$ ). P1 represents cells containing polarized mitochondria. (A, B) Plots for the negative control; (C–F) plots of 1A fractions showing no pattern of early and late apoptotic cell populations; (G–L) plots of 2AFH fractions showing a pattern of early and late apoptotic cell populations

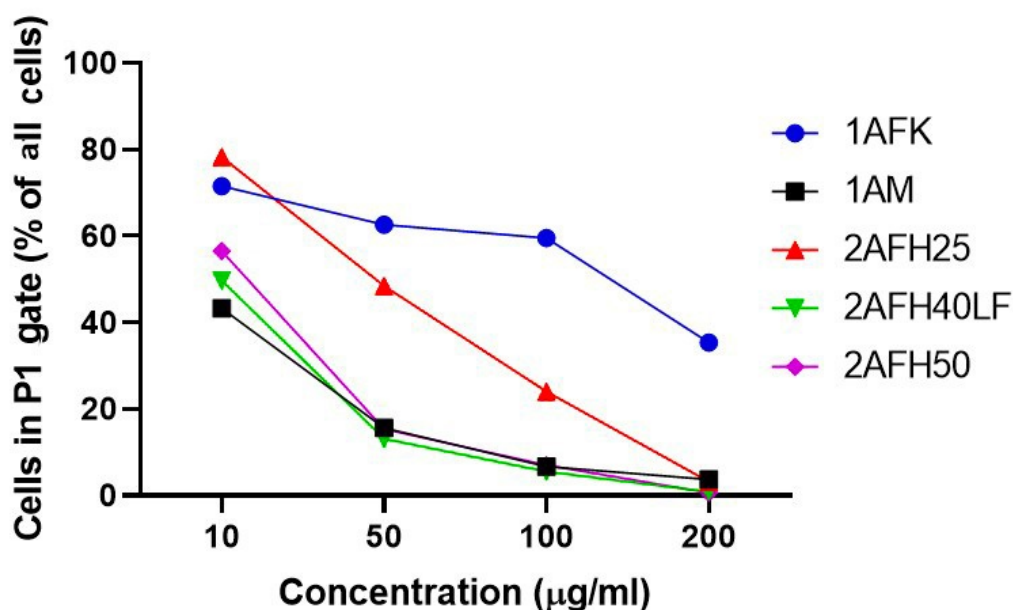


**Figure 9.** Average proportions of HeLa cells in P1 gate after 4 h treatment with extract fractions 1AFK, 1AM, 2AFH25, 2AFH40LF and 2AFH50 and staining with JC-1

The plot of  $\Delta\Psi_M$  (as a percentage of the  $\Delta\Psi_M$  for the negative control) versus concentration, following treatment with each of the five extract fractions, is shown in Figure 10. All extract fractions reduced  $\Psi_M$  in a concentration-dependent manner. With respect to 1A fractions, 1AFK reduced  $\Psi_M$  significantly at 200  $\mu\text{g}/\text{mL}$  ( $P < 0.01$ ), while 1AM caused significant reductions ( $P < 0.01$  or  $P < 0.001$ ) at all of its concentrations. With regard to the 2AFH fractions 2AFH25, 2AFH40LF and 2AFH50, each showed a significant reduction ( $P < 0.05$  or  $P < 0.01$ ) in  $\Psi_M$  at each of its concentrations tested, except 10  $\mu\text{g}/\text{mL}$ .

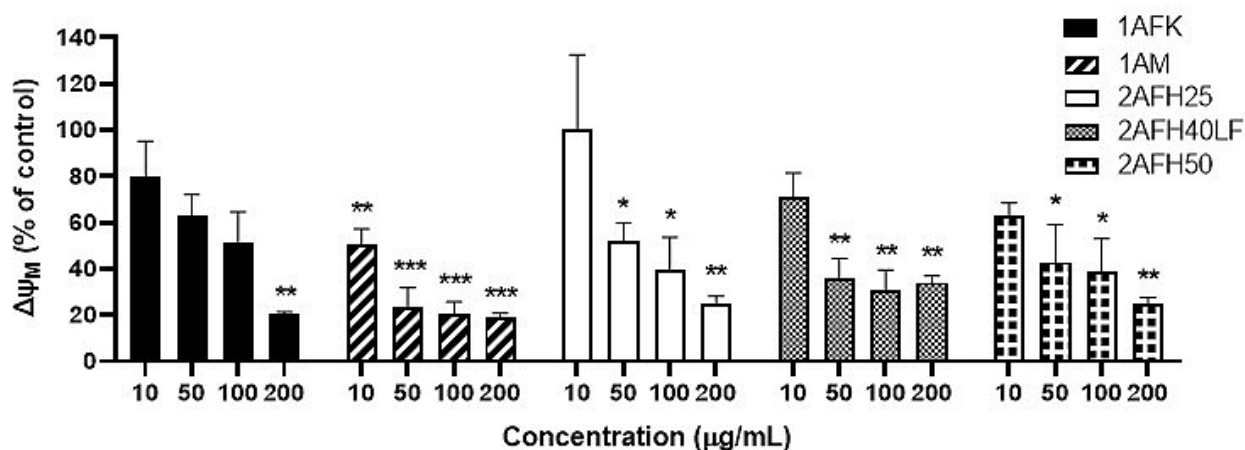


**Figure 10.** Effects of extract fractions 1AFK, 1AM, 2AFH25, 2AFH40LF and 2AFH50 on the  $\Delta\Psi_M$  in HeLa cells. Each value is expressed as a percentage of the  $\Delta\Psi_M$  for the negative control. \*  $P < 0.05$ , \*\*  $P < 0.01$  and \*\*\*  $P < 0.001$  compared to the negative control

### Components of 2AFH50 identified by GC-MS

GC-MS identified 16 compounds in 2AFH50, with the most abundant components being fatty acids with retention times ranging between 9.930 min and 21.462 min. Based on proportion in the fraction, the top five components are *n*-hexadecanoic acid (52.29%), decanoic acid 10-(2-hexylcyclopropyl) (10.78%), octadecanoic acid (8.48%), 24S-Ethyl-5.alpha.-cholesta-2, 22E-dien-6-one (5.26%), and stigmasta-3,5-dien-7-one (3.24% + 2.17%). The components of 2AFH50 identified by GC-MS are shown in Table 3.

**Table 3.** Compounds identified in fraction 2AFH50 via GC-MS

Components of 2AFH50	RT (min)	Qual %	Area %	MM (g/mol)
2,4-Di- <i>tert</i> -butylphenol	9.930	94	1.05	206.32
Tetradecanoic acid	12.808	97	1.59	228.37
2-Pentadecanone, 6,10,14-trimethyl-	13.585	80	1.29	268.50
<i>n</i> -Hexadecanoic acid	14.996	99	52.29	256.40
Heptadecanoic acid	15.763	91	1.42	270.45
13-Tetradecene-11-yn-1-ol	16.107	59	1.37	208.34
1,6-Dimethyl-9-(1-methylethylidene)-5,12-dioxatricyclo[9.1.0.0(4,6)]dodecan-8-one	16.420	49 <sup>a</sup>	1.63	250.33
Octadecanoic acid	16.696	99	8.48	284.48
2,2,4a,6a,8a,9,12b,14a-Octamethyl-1,2,3,4,4a,5,6,6a,6b,7,8,8a,9,12,12a,12b,13,14,14a,14b-eicosahydricene	17.218	46 <sup>a</sup>	1.58	410.70
Decanoic acid, 10-(2-hexylcyclopropyl)	17.429	99	10.78	296.49
1,4-Dioxaspiro[4.5]decane-6-carboxylic acid, dimethylamide	18.218	89	2.10	213.27
Cholesta-8,24-dien-3-ol, 4-methyl-, (3.β.,4.α.)-	19.174	90	1.20	398.70
A-Norcholestan-3-one, 5-ethenyl-, (5.β.)-	19.251	41 <sup>a</sup>	2.47	398.50
24S-Ethyl-5.α.-cholesta-2,22E-dien-6-one	20.784	64	5.26	410.70
Stigmasta-3,5-dien-7-one	21.273	70	5.41	410.68
2H-3,9a-methano-1-benzoxepin, octahydro-2,2,5a,9-tetramethyl-[3R-(3.α.,5a.α.,9.α.,9a.α.)]-	21.462	50	2.07	222.37

Area %: area percent, which corresponds to the proportion of each component in the fraction; Qual %: quality of fragment ion peak matching between the unknown component and suggested compounds from NIST14.L; RT: retention time in min; MM: molecular mass. The “a” in superscript represents suggested compounds from NIST14.L which have Qual % less than 50%

## Discussion

The epicarp of tropical fruits has been reported to contain numerous phytochemicals which have been harnessed for human use in the pharmaceutical industries and in traditional medicine [24, 25]. Ajayi et al. [22] reported the potential protein targets of drug-like compounds from fractions of ethanol extract of the epicarp of *C. rostrata* and submitted that the epicarp contains phytochemicals with potential against pain and inflammatory diseases, diabetes and cancer. This study investigated the anti-proliferative and cytotoxic potential of the crude ethanol extract from the epicarp (1A) and ethanol extract of the leaf of *C. rostrata* (2A) against cancer cell lines: HeLa and MRC5-SV2.

1A showed significant cytotoxicity against both cell lines, but the effect was not time-dependent against HeLa or MRC5-SV2 cells. The cytotoxicity of the extract against HeLa was highest at the 50 µg/mL treatment. While the reason for this pattern was not entirely clear, it could be that at higher concentrations of 1A the perturbation of metabolic pathways in HeLa cells induced mechanisms that attenuated the effects, e.g., increased expression of transporters to pump out the phytochemicals [26]. The lack of additional cytotoxic effect at a longer time point could also be attributable to the nature of the cytotoxic components in the extract, e.g., their half-life in growth medium, their interactions with cellular components of dying cells or their interactions with normal waste products of cultured cell metabolism [27, 28]. The IC<sub>50</sub> values for the cytotoxicity of 1A show that MRC5-SV2 cells are slightly more sensitive to the effect of the extract than HeLa cells.

The fractionation of 1A through solvent partitioning produced two fractions, 1AFK and 1AM, both of which showed lower cytotoxicity against both cell lines at 48 h. This suggests that, in 1A, the cytotoxic contents of the fractions had synergized with one another, resulting in lower IC<sub>50</sub> values for the cytotoxicity of 1A against the two cell lines, following 48 h treatment, compared to the separate fractions producing IC<sub>50</sub> values that were significantly higher against HeLa and MRC5-SV2 cells over the same exposure time. The effect of 1AFK on the cells involved the formation of pore-like damage on the cell membrane at 50 µg/mL and 100 µg/mL and it also induced significant oxidative stress and depolarization of the mitochondrial membrane (impairment of mitochondrial health). The findings suggest 1AM might act through other means than the generation of ROS, as it induced less than 2-fold increase in ROS. Data from the JC-1 staining assay

also suggest that 1AM induces apoptosis (1AM was even more potent than 1AFK in reducing  $\Delta\Psi_M$ ), which could be through means such as inhibition of intracellular antioxidant enzyme systems. It is also possible that, in some cases, lytic events were part of the cytotoxic response.

The leaf ethanol extract, 2A, showed significant cytotoxic activity against HeLa and MRC5-SV2 cells at 48 h, with  $IC_{50}$  values of  $148.0 \mu\text{g/mL} \pm 4.8 \mu\text{g/mL}$  and  $165.0 \mu\text{g/mL} \pm 8.8 \mu\text{g/mL}$ , respectively. Fractionation of the crude extract by solvent partitioning, VLC and column chromatography produced non-polar fractions (2AFU and 2AFH) with increased cytotoxicity, while the methanol fraction (2AFM), which had the highest proportion by mass in the crude, was less cytotoxic. A previous study on the leaf of *C. lepidota* (a close variety) by Oghenerobo and Falodun [29] reported high DPPH radical-scavenging activity of the chloroform and methanol extracts. The relatively non-cytotoxic effect of 2AFM is consistent with the findings of Oghenerobo and Falodun [29], and a high antioxidant activity may be the rationale for its low cytotoxicity. While the mechanism of action of fraction 2AFU only involved a mild increase in ROS levels, the effects of the cytotoxic sub-fractions (2AFH25, 2AFH40LF and 2AFH50) obtained from the 2AFH fraction involved several-fold increases in ROS levels and/or impairment of mitochondrial activity as demonstrated by reduced  $\Delta\Psi_M$ .

The GC-MS analysis of 2AFH50 identified saturated short- to medium-chain natural fatty acids as the major components; the proportion of palmitic acid (hexadecanoic acid) in 2AFH50 was 52%. Free fatty acids have been reported to disrupt the membrane architecture of human erythrocytes, affecting membrane fluidity and membrane protein functions [30]. A high concentration of palmitic acid has been reported to affect the membrane permeability of Caco-2 cells without inducing cytotoxicity or oxidative stress [31]. Increased incorporation of medium-chain fatty acids present in the extract into the membranes of HeLa and MRC5-SV2 cells might have sensitized the cells to the cytotoxic effects of other components in the extract. Palmitic acid was found to increase the production of nitric oxide in primary cultured rat skeletal muscle cells, and nitric oxide contributes to oxidative stress in many cells, including neurons [32, 33]. Though the effect of free palmitic acid on the viability of HeLa and MRC5-SV2 cells has not been investigated, literature reports support the argument that palmitic acid might have contributed to the cytotoxicity of 2AFH50 against HeLa and MRC5-SV2 cells.

In conclusion, cancer is a major public health challenge that necessitates the development of more efficacious and safer chemotherapeutic drugs. This work identifies *C. rostrata* as a potential source of new anti-cancer agents and further highlights the need to extensively screen more plants for bioactive principles that might represent novel scaffolds and deliver new chemical leads for drug discovery and development. Such endeavours can also produce fingerprints for the complex extracts and fractions which can be useful for quality control and authentication purposes, thus helping to achieve the standardisation necessary for the integration of traditional medicine into mainstream healthcare.

## Abbreviations

$\Delta\Psi_M$ : mitochondrial membrane potential

DCFDA: 2',7'-dichlorofluorescein diacetate

DMSO: dimethyl sulfoxide

GC-MS: gas chromatography-mass spectrometry

JC-1: 5,5',6,6'-tetrachloro-1,1',3,3'-tetraethyl-imidacarbocyanine iodide

MTT: 3-(4,5-dimethylthiazol-2-yl)-2,5-diphenyltetrazolium bromide

NIST: National Institute of Standards and Technology

PBS: phosphate-buffered saline

ROS: reactive oxygen species

TBHP: tert-butyl hydroperoxide

VLC: vacuum liquid chromatography

## Declarations

### Acknowledgments

The Centre for Natural Products Discovery (CNPD), School of Pharmacy and Biomolecular Sciences, Liverpool John Moores University, UK is gratefully acknowledged for the access to instruments, resources, and training provided BEA while he conducted the research at the centre as a visiting PhD student between June and October 2019, hosted by AAF and supervised by AAF, SDS and DWS.

### Author contributions

BEA: Data curation, Formal analysis, Funding acquisition, Investigation, Methodology, Validation, Visualization, Writing—original draft, Writing—review & editing. BO: Conceptualization, Supervision, Writing—review & editing. JBM: Conceptualization, Supervision, Writing—review & editing. DWS: Formal analysis, Investigation, Methodology, Supervision, Validation, Writing—review & editing. SDS: Methodology, Resources, Supervision, Validation, Writing—review & editing. AAF: Conceptualization, Data curation, Formal analysis, Funding acquisition, Investigation, Methodology, Project administration, Resources, Supervision, Validation, Visualization, Writing—review & editing. All authors read and approved the manuscript.

### Conflicts of interest

The authors declare that they have no conflicts of interest.

### Ethical approval

Not applicable.

### Consent to participate

Not applicable.

### Consent to publication

Not applicable.

### Availability of data and materials

Datasets are available from the authors upon reasonable request. Contact [tobitune@yahoo.com](mailto:tobitune@yahoo.com) or [A.A.Fatokun@ljmu.ac.uk](mailto:A.A.Fatokun@ljmu.ac.uk).

### Funding

The work described in this manuscript was partly supported by a Seed Corn Grant (2017) awarded to AAF by Liverpool John Moores University (LJMU). This funder had no role in study design, data collection and analysis, decision to publish, or preparation of the manuscript.

### Copyright

© The Author(s) 2023.

## References

1. Hanahan D, Weinberg RA. Hallmarks of cancer: the next generation. *Cell*. 2011;144:646–74.
2. American Cancer Society. Cancer prevention & early detection facts & figures 2021-2022. Atlanta: American Cancer Society; 2021.
3. Sung H, Ferlay J, Siegel RL, Laversanne M, Soerjomataram I, Jemal A, et al. Global cancer statistics 2020: GLOBOCAN estimates of incidence and mortality worldwide for 36 cancers in 185 countries. *CA Cancer J Clin*. 2021;71:209–49.
4. Huang CY, Pai YC, Yu LC. Glucose conferred irinotecan chemoresistance through divergent actions of pyruvate and ATP in cell death and proliferation of colorectal cancer. *Oncology*. 2022;100:555–68.

5. Newman DJ, Cragg GM. Natural products as sources of new drugs over the nearly four decades from 01/1981 to 09/2019. *J Nat Prod.* 2020;83:770–803.
6. Balunas MJ, Kinghorn AD. Drug discovery from medicinal plants. *Life Sci.* 2005;78:431–41.
7. Ibekwe NN, Ameh SJ. Plant natural products research in tuberculosis drug discovery and development: a situation report with focus on Nigerian biodiversity. *Afr J Biotechnol.* 2014;13:2307–20.
8. Atanasov AG, Waltenberger B, Pferschy-Wenzig EM, Linder T, Wawrosch C, Uhrin P, et al. Discovery and resupply of pharmacologically active plant-derived natural products: a review. *Biotechnol Adv.* 2015;33:1582–614.
9. Ngulde SI, Sandebe UK, Hussaini IM. Ethnobotanical survey of anticancer plants in Askira/Uba local government area of Borno State, Nigeria. *Afr J Pharm Pharmacol.* 2015;9:123–30.
10. Hao DC, Xiao PG. Pharmaceutical resource discovery from traditional medicinal plants: pharmacophylogeny and pharmacophylogenomics. *Chin Herb Med.* 2020;12:104–17.
11. Gonmadje CF, Doumenge C, Sunderland TCH, Balinga MPB, Sonké B. Phytogeographical analysis of Central African forests: the Ngovayang massif (Cameroon). *Plant Ecol Evol.* 2012;145:152–64.
12. Odion EE, Poh CF, Falodun A, Adelusi SA. *Cola rostrata*: phytochemical and toxicity studies. *J Appl Sci Environ Manage.* 2013;17:603–7.
13. Libalah MB, Droissart V, Sonké B, Hardy OJ, Drouet T, Pescador DS, et al. Shift in functional traits along soil fertility gradient reflects non-random community assembly in a tropical African rainforest. *Plant Ecol Evol.* 2017;150:265–78.
14. Dunn J, Agom D. Tree use in Igonigoni and Abo Mkpang, Cross River State, Nigeria; a comparison of two villages located in areas with different vegetation types. *Global Ecol Biogeogr Lett.* 1992;2:196–206.
15. Essien EE, Peter NS, Akpan SM. Chemical composition and antioxidant property of two species of Monkey kola (*Cola rostrata* and *Cola lepidota* K. Schum) extracts. *European J Med Plants.* 2015;7:31–7.
16. Christopher GI, Ogundu EC, Umoren UE, Udofe MJ. Performance of growing African Giant Snails (*Archachatina marginata*) fed forage mixtures and maize-based concentrate supplemented with Monkey Cola (*Cola rostrata*) seed meal. *Asian J Adv Agric Res.* 2019;8:1–7.
17. Cheek M. Three new species of *Cola* (Sterculiaceae) from western Cameroon. *Kew Bull.* 2002;57:403–15.
18. Engel N, Oppermann C, Falodun A, Kragl U. Proliferative effects of five traditional Nigerian medicinal plant extracts on human breast and bone cancer cell lines. *J Ethnopharmacol.* 2011;137:1003–10.
19. Mbaveng AT, Manekeng HT, Nguenang GS, Dzotam JK, Kuete V, Efferth T. Cytotoxicity of 18 Cameroonian medicinal plants against drug sensitive and multi-factorial drug resistant cancer cells. *J Ethnopharmacol.* 2018;222:21–33.
20. Odion EE, Engel N, Falodun A, Adelusi SA. Phytochemical screening, antiproliferative and apoptotic activities of the root bark extract and fractions of *Cola rostrata* (Sterculiaceae) K. Schum. in MCF-7 cell line. *J Sci Pract Pharm.* 2020;6:337–43.
21. Ebana RUB, Etok CA, Edet UO. Chemical composition and antimicrobial analysis of the pods and seeds of *Cola rostrata* and *Cola nitida*. *Int J Innovation Appl Stud.* 2015;10:1245–50.
22. Ajayi BE, Oboh B, Minari JB, Fatokun AA. *In silico* identification of protein targets for drug-like compounds from epicarp extract of *Cola rostrata* K. Schum. *J Appl Sci Environ Manage.* 2022;26:903–11.
23. Omondi RO, Bellam R, Ojwach SO, Jaganyi D, Fatokun AA. Palladium (II) complexes of tridentate bis(benzazole) ligands: structural, substitution kinetics, DNA interactions and cytotoxicity studies. *J Inorg Biochem.* 2020;210:111156.
24. Fakayode OA, Abobi KE. Optimization of oil and pectin extraction from orange (*Citrus sinensis*) peels: a response surface approach. *J Anal Sci Technol.* 2018;9:20.



25. Zioga M, Chroni A, Evageliou V. Utilisation of pectins extracted from orange peels by non conventional methods in the formation of edible films in the presence of herbal infusions. *Polysaccharides*. 2022;3: 574–88.
26. Wu J, Lin N, Li F, Zhang G, He S, Zhu Y, et al. Induction of P-glycoprotein expression and activity by *Aconitum* alkaloids: implication for clinical drug–drug interactions. *Sci Rep*. 2016;6:25343.
27. Arodin Selenius L, Wallenberg Lundgren MW, Jawad R, Danielsson O, Björnstedt M. The cell culture medium affects growth, phenotype expression and the response to selenium cytotoxicity in A549 and HepG2 cells. *Antioxidants (Basel)*. 2019;8:130.
28. Palombo P, Bürkle A, Moreno-Villanueva M. Culture medium-dependent isoproterenol stability and its impact on DNA strand breaks formation and repair. *Chem Biol Interact*. 2022;357:109877.
29. Oghenerobo VI, Falodun A. Antioxidant activities of the leaf extract and fractions of *Cola lepidota* K. Schum (sterculiaceae). *Niger J Biotechnol*. 2013;25:31–6.
30. Lapshina EA, Zavodnik IB, Bryszewska M. Effect of free fatty acids on the structure and properties of erythrocyte membrane. *Scand J Clin Lab Invest*. 1995;55:391–7.
31. Gori M, Altomare A, Cocca S, Solida E, Ribolsi M, Carotti S, et al. Palmitic acid affects intestinal epithelial barrier integrity and permeability *in vitro*. *Antioxidants (Basel)*. 2020;9:417.
32. Wei T, Chen C, Hou J, Xin W, Mori A. Nitric oxide induces oxidative stress and apoptosis in neuronal cells. *Biochim Biophys Acta*. 2000;1498:72–9.
33. Lambertucci RH, Leandro CG, Vinolo MA, Nachbar RT, Dos Reis Silveira L, Hirabara SM, et al. The effects of palmitic acid on nitric oxide production by rat skeletal muscle: mechanism via superoxide and iNOS activation. *Cell Physiol Biochem*. 2012;30:1169–80. Erratum in: *Cell Physiol Biochem*. 2013; 31:14.